bandwidth and intensity of the $-CH_2-$ stretching bands, the appearance of the 1415-cm^{-1} band in the $-CH_2-$ bending region of the Raman spectrum, and the splitting observed in the IR spectra at low temperature. A phase transition having many structural similarities has been recently observed in the *n*-alkane clathrates[21] where at low temperature a contraction of the urea lattice increases the intermolecular interaction between *n*-alkane chains, thus also changing the subcell structure.

The exact mechanism of the transition is unclear, but an analogy to that observed by Zerbi et al.[20] for *n*-alkanes may not be drawn due to the thermodynamic incompatibility of hydrocarbon and fluorocarbon chains. Any surface disordering mechanism in the F12H10F12 triblock crystals would involve the longitudinal motion of fluorocarbon segments through a hydrocarbon lattice, which is highly unlikely due to the incompatible nature of these chemical species.

Thus, it has been shown that the F12H10F12 triblock molecule exists in a hexagonal-like structure at room temperature similar to that found for odd *n*-alkanes a few degrees below their melting point. At low temperatures, the F12H10F12 undergoes a transition to a new phase characterized by a decrease in molecular mobility due to an increase in the intermolecular coupling. Spectral observations indicate that this new phase is similar to the orthorhombic phase that exists in the odd *n*-alkanes at room temperature. No specific information was obtained from the Raman spectra of the fluorocarbon portion of the molecule to suggest that it has undergone a conformational change at low temperature, although here some subtle change to allow closer proximity of the hydrocarbon segments may not be spectroscopically detectable. Future studies will address this aspect in more detail.

Acknowledgment. We acknowledge the financial support and technical motivation of L. Siperko and D. Barr of the IBM Endicott Laboratories.

References and Notes

(1) Broadhurst, M. G. *J. Res. Natl. Bur. Stand.* **1962,** *66A,* 241.
(2) Vanni, H.; Rabolt, J. F. *J. Polym. Sci., Polym. Phys. Ed.* **1980,** *18,* 587.
(3) Martin, G. M.; Eby, R. K. *J. Res. Natl. Bur. Stand.* **1968,** *72A,* 467.
(4) Miller, R. D.; Hofer, D.; Rabolt, J. F.; Fickes, G. N. *J. Am. Chem. Soc.* **1985,** *107,* 2172.
(5) Tatsumi, T.; Fukushima, T.; Imada, K.; Takayanagi, M. *J. Macromol. Sci., Phys.* **1967,** *B1,* 459.
(6) Bridgman, P. W. *Proc. Am. Acad. Arts Sci.* **1948,** *76,* 71.
(7) Rabolt, J. F.; Piermarini, G.; Block, S. *J. Chem. Phys.* **1978,** *69,* 2872.
(8) Rabolt, J. F.; Russell, T. P.; Twieg, R. J. *Macromolecules* **1984,** *17,* 2786.
(9) Russell, T. P.; Rabolt, J. F.; Twieg, R. J.; Siemens, R. L.; Farmer, B. L. *Macromolecules* **1986,** *19,* 1135.
(10) Viney, C.; Russell, T. P.; Depero, L. E.; Twieg, R. J. *Mol. Cryst. Liq. Cryst.* **1989,** *168,* 63.
(11) Viney, C.; Twieg, R. J.; Russell, T. P.; Depero, L. E. *Liq. Cryst.* **1989,** *5,* 1783.
(12) Twieg, R. J.; Rabolt, J. F. *Macromolecules* **1988,** *21,* 1806.
(13) Boerio, F. J.; Koenig, J. L. *J. Chem. Phys.* **1970,** *52,* 4826.
(14) Rabolt, J. F.; Fanconi, B. *Macromolecules* **1978,** *11,* 740.
(15) Hendra, P. J.; Jobic, H. P.; Marsden, E. P.; Bloor, D. *Spectrochim. Acta* **1977,** *33A,* 445.
(16) Olf, H.; Fanconi, B. *J. Chem. Phys.* **1973,** *59,* 534.
(17) Barnes, J. D.; Fanconi, B. *J. Chem. Phys.* **1972,** *56,* 5190.
(18) Snyder, R. J.; Hsu, S. L.; Krimm, S. *Spectrochim. Acta* **1978,** *34A,* 395.
(19) Zerbi, G.; Roncone, P.; Longhi, G.; Wunder, S. L. *J. Chem. Phys.* **1988,** *89,* 166.
(20) Zerbi, G.; Magni, R.; Gussoni, M.; Moritz, K. H.; Bigotto, A.; Dirlikov, S. *J. Chem. Phys.* **1981,** *75,* 3175.
(21) Casal, H. L.; Cameron, D. G.; Kelusky, E. C. *J. Chem. Phys.* **1984,** *80,* 1407.

K. Song, R. J. Twieg, and J. F. Rabolt*

IBM Research Division, Almaden Research Center
650 Harry Road, San Jose, California 95120-6099

Received March 5, 1990
Revised Manuscript Received May 30, 1990

Enhanced Stability and Facilitation in the Oxygen Transport through Cobalt Porphyrin Polymer Membranes

We describe herein the polymer-bound cobalt porphyrin derivatives with large oxygen-binding kinetic constants and with extraordinarily prolonged lifetimes through which oxygen permeates with high selectivity ($P_{O_2}/P_{N_2} > 10$).

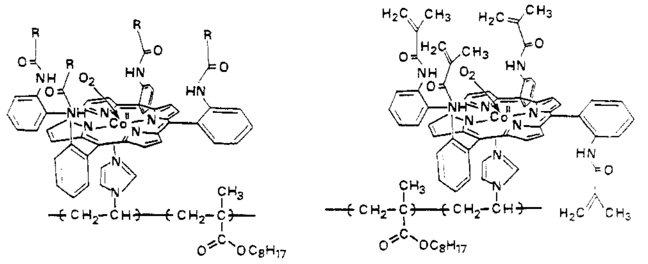

1a 4R = $-C(CH_3)_3$

1b 3R = $-C(CH_3)_3$ 1R = $-\overset{CH_3}{C}=CH_2$

1c 2R = $-C(CH_3)_3$ 2R = $-\overset{CH_3}{C}=CH_2$

2

Metalloporphyrin and cobalt–Schiff base chelates with oxygen-binding ability have been applied to an oxygen-transporting fluid[1] and to an oxygen-enriching liquid membrane.[2] But these oxygen-carrying metal chelates in solutions are often irreversibly oxidized and their lifetimes as an oxygen carrier are quite limited. We have recently reported measurements of facilitated oxygen transport in dry (or solvent-free) polymer membranes containing a cobalt porphyrin and a cobalt–Schiff base chelate as a fixed carrier which sorbs oxygen selectively and reversibly.[3] We intended here to enhance the efficiency of this facilitated transport and to prolong the lifetime of the metal chelate as an oxygen carrier. We synthesized the following polymer-bound cobalt porphyrins: *meso*-mono(α-*o*-methacrylamidophenyl)tris(α,α,α-*o*-pivalamidophenyl)-

0024-9297/90/2223-3714$02.50/0

Table I
Oxygen-Binding Equilibrium Constant, Thermodynamic and Kinetic Parameters, and Dual-Mode Transport Parameters for the CoP Membranes at 45 °C

						diffusion coeff, cm^2/s			
complex	$10^{-3}K$, 1/M	ΔH, kcal/mol	ΔS, eu	$10^{-7}k_{on}$,[b] 1/M·s	$10^{-3}k_{off}$,[b] 1/s	10^6D_{DD}	10^7D_{DC}	10^8D_{CD}	10^9D_{CC}
1a	3.0	−13	−37	0.98	3.2	2.2	0.97	0.86	3.1
1b	4.3	−13	−37	1.4	3.2	2.2	2.2	1.5	7.3
1c	4.0	−13	−38	2.3	5.7	2.3	2.6	2.0	9.0
2	0.51	−11	−36	3.4	66	2.2	3.2	22	144

[a] $10^3k_D(cm^3(STP)/cm^3\ cmHg) = 7.2 \pm 0.1$; $C_C'(cm^3(STP)/cm^3) = 0.2$; CoP content = 1.3 wt %. [b] 20 °C.

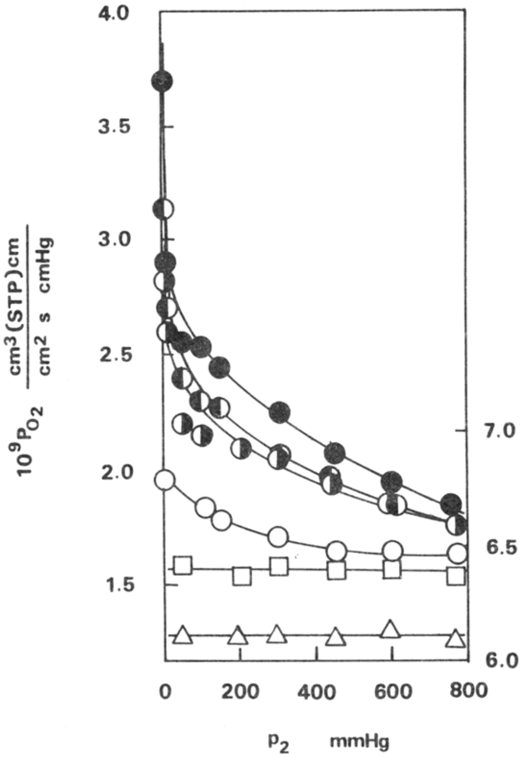

Figure 1. Effect of upstream gas pressure (p_2) on the permeability coefficient for the CoP membranes at 45 °C. Oxygen: **1a** (○), **1b** (◑), **1c** (◐), **2** (●), and $Co^{III}P$ (□). Nitrogen: **2** (▲).

porphinatocobalt (**1b**), *meso*-bis(α,α-*o*-methacrylamidophenyl)bis(α,α-*o*-pivalamidophenyl)porphinatocobalt (**1c**), and *meso*-tris(α,α,α-*o*-methacrylamidophenyl)mono-(β-*o*-methacrylamidophenyl)porphinatocobalt (**2**). These polymers are new derivatives of the well-known *meso*-tetra(α,α,α,α-*o*-pivalamidophenyl)porphinatocobalt (**1a**). Rubbery transparent membranes were prepared by coordinating the cobalt porphyrin (CoP) to poly(octyl methacrylate-*co*-vinylimidazole)[4] and then casting films from chloroform solutions of these polymers. The imidazole residue of the polymer coordinates to the fifth coordination site of CoP, and the sixth coordination site is vacant, even in the solid membrane, to bind oxygen rapidly and reversibly. We describe in this paper the effects of polymer-bound CoP structure on the lifetime of oxygen-binding ability, the oxygen-binding kinetic constants, and the facilitated oxygen transport in the membrane and discuss the oxygen-transport mechanism by a dual-mode transport model.

The UV–visible absorption spectra of the deoxy-CoP membranes in vacuo were changed to the spectra assigned to the oxy-CoP (Co/O_2 = 1:1) on exposure air.[5] This change was completed within several seconds for a 10-μm-thick membrane. This observation implies that the oxygen-binding and -dissociation reaction kinetics are rapid.

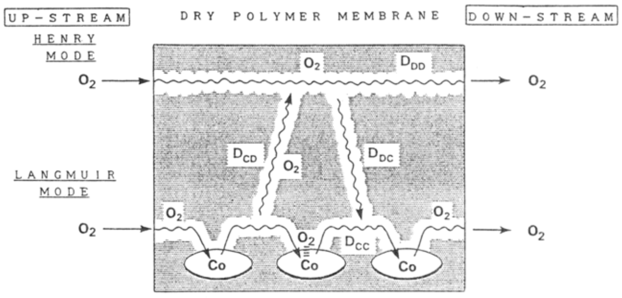

Figure 2.

The deoxy–oxy cycle was repeated at 1-min intervals and recorded 1.2 × 10^5 times (ca. 6 mo) by changing the atmosphere of the membrane from reduced pressure (ca. 20 mmHg) to laboratory air pressure (760 mmHg) at 25 °C. The CoP coordinated to low molecular weight imidazole and dispersed physically in poly(octyl methacrylate) membrane irreversibly oxidized during the deoxy–oxy cycles. Lifetimes (half-life period of the oxygen-binding ability) for the monomeric imidazole–CoP's, **2**, **1c**, and **1a** were less than 10 h, approximately 15 h, and about 20 days, respectively. In contrast to the monomeric CoP's, the lifetimes for the polymer-bound CoP's were much longer; for **2**, **1c**, and **1a**, the lifetimes were approximately 13 days, 15 days, and more than 2 mo, respectively. When the CoP is fixed on the polymer chain, it strikingly inhibits the irreversible oxidation[6] and maintains its oxygen-binding ability for over a month's working.

Photodissociation and recombination of bound oxygen to and from CoP in the membrane were observed by laser flash photolysis.[7] For example, the reaction for the **2** membrane was completed within 100 μs, and it is a surprisingly rapid reaction. The oxygen-binding and -dissociation rate constants (k_{on} and k_{off}, respectively) were estimated by pseudo-first-order kinetics and are shown in Table I. The CoP's are kinetically active for oxygen binding even after immobilization in the dry polymer membranes. k_{on} and k_{off} for **1c** and **2** are much larger than those for **1a**. This result indicates that the porphyrin structure clearly influences the oxygen-binding character of CoP and that reduction in the steric hindrance on the porphyrin plane or the oxygen-binding and -dissociation pathway enhances the rate constants k_{on} and k_{off}. The combination of CoP with the polymer in the dry-membrane state prolongs the lifetime of CoP for oxygen binding and enables precise spectroscopic measurement of the oxygen-binding reaction parameters.

Figure 1 shows the permeability coefficient of oxygen and nitrogen (P_{O_2} and P_{N_2}) for the CoP membranes.[8] P_{N_2} is smaller than P_{O_2} and independent of upstream nitrogen pressure, $p_2(N_2)$ because the fixed carrier, CoP, does not bind with nitrogen. P_{O_2} is also small and independent of upstream oxygen pressure, $p_2(O_2)$, for the membrane composed of the inert $Co^{III}P$, which does not interact with oxygen. On the other hand, P_{O_2} is much larger than P_{N_2} for the active CoP membranes and increases with the decrease in $P_2(O_2)$. These observations suggest that the CoP in the membrane interacts with oxygen and facilitates the oxygen transport in the membrane. In particular, P_{O_2} values for the **1c** and **2** membrane steeply increase at low $p_2(O_2)$ as shown in Figure 1. The permeability ratio (P_{O_2}/P_{N_2}) at $p_2(O_2)$ = 5 mmHg was 5.8 and 12 for the membranes containing 1.3 and 5 wt % **2**, respectively.

This facilitated oxygen transport in the CoP polymer membranes is considered to occur by a dual-model transport mechanism (Henry mode and Langmuir mode; Figure 2). The dual-mode transport model is given as follows.[9-11]

$$P = k_D D_{DD} + \frac{C_C' K D_{CC}}{(1 + Kp_2)} + \left[\frac{C_C' K D_{CD} - k_D D_{DC}}{(1 + Kp_2)} + \frac{2k_D D_{DC}}{Kp_2} \ln(1 + Kp_2) \right] \quad (1)$$

That is, P is equal to the sum of the first term, which represents the Henry's law mode attributed to a physical permeation through a polymer matrix, the second term for the Langmuir mode attributed to a specific binding and diffusion of oxygen to and via the fixed oxygen carrier CoP, and the third term, which is also the Langmuir mode attributed to the exchange between the first and second terms. Here, k_D is the physical solubility coefficient for the Henry's law mode. D_{DD}, D_{DC}, D_{CD}, and D_{CC} are the diffusion coefficients for the Henry's law physical permeation, for the diffusion from the polymer matrix to the fixed carrier, for the diffusion from the fixed carrier to the polymer matrix, and for hopping between the fixed carriers, respectively. C_C' is the fixed carrier CoP concentration in the membrane.

The experimental data in Figure 1 were analyzed by the dual-mode transport model and gave the parameters listed in Table I. D_D and k_D values agree with each other for the CoP membranes containing **1a–c** and **2** and with those determined for the inert Co^{III}P membrane. This result means that the polymer matrix is not influenced by the CoP loading and supports the calculation procedure based on eq 1. The oxygen diffusion coefficients in Table I suggest the following: (i) The reaction rate constants, k_{on} and k_{off}, determined spectroscopically for oxygen-binding and -dissociation to and from the CoP as a fixed oxygen carrier, are clearly related to the diffusion coefficients D_{DC} and D_{CD} determined from the transport measurement. (ii) The ratio D_{CC}/D_{DD} shows that the diffusion constant, postulated in Figure 2 for the hopping pathway of oxygen between the fixed carriers, is approximately one-tenth of that of the physical permeation in the membrane. (iii) The CoP carriers, **1c** and **2**, with larger k_{on} and k_{off}, give larger D_{DC}, D_{CD}, and D_{CC} and bring about highly efficient facilitation in the oxygen transport.

Acknowledgment. This work was partially supported by a Grant-in-Aid for Scientific Research from the Ministry of Education, Science, and Culture, Japan.

References and Notes

(1) Tsuchida, E.; Nishide, H. *Top. Curr. Chem.* **1986**, *132*, 63.

(2) Jonson, B. M.; Baker, R. W.; Matson, S. L.; Smith, K. L.; Roman, I. C.; Tuttle, M. K.; Lonsdale, H. K. *J. Membr. Sci.* **1987**, *31*, 31.

(3) (a) Nishide, H.; Ohyanagi, M.; Okada, O.; Tsuchida, E. *Macromolecules* **1986**, *19*, 444. (b) Nishide, H.; Ohyanagi, M.; Kawakami, H.; Okada, O.; Tsuchida, E. *Macromolecules* **1987**, *20*, 417, 1907. (c) Nishide, H.; Ohyanagi, M.; Okada, O.; Tsuchida, E. *Macromolecules* **1988**, *21*, 2910.

(4) Poly(octyl methacrylate-*co*-vinylimidazole) was prepared by the radical copolymerization of octyl methacrylate and *N*-vinylimidazole initiated by azobis(isobutyronitrile). The vinylimidazole residue content and the molecular weight of the copolymer were determined to be 3.3 mol % and 1.7 × 10^6, by elemental analysis and gel permeation chromatography (with tetrahydrofuran as the solvent and polystyrene as the standard), respectively. The chloroform solution of the polymer and CoP was carefully cast onto a Teflon plate in an oxygen-free atmosphere, followed by drying in vacuo, to yield a transparent, wine red membrane with a thickness of 60 μm and containing 1.3 wt % CoP.

(5) λ_{max}(deoxy) 528 nm, λ_{max}(oxy) 546 nm, and isosbestic points at 480, 537, and 667 nm, for the deoxy–oxy alternation. No difference was observed in the UV–visible absorption spectra of **1a–c** and **2**.

(6) It is known that the oxy-CoP forms with another deoxy-CoP, a μ-dioxy-CoP, which is converted irreversibly to Co^{III}P without oxygen-binding ability.

(7) The laser flash was applied perpendicularly to the light path of a rapid and sensitive spectrophotometer (Unisoku FR-2000), and the membrane was placed at the crossing of the laser flash and the light path and at 45 °C to both. The rapid UV absorption change was recorded with the spectrophotometer using a kinetic data processer to cancel the noise caused by scattered light.

(8) Oxygen permeation coefficients for various upstream gas pressures were measured with a low-vacuum permeation apparatus in the chamber with stable thermostating (Rika Seiki Inc. Model K-315 N-01). The pressures on the upstream and downstream sides were detected by using a Baratron absolute pressure gauge (MKS Instruments Inc.). Nitrogen permeation coefficients were measured by the same procedure as for oxygen. The permeation coefficients were calculated from the slope of the steady-state straight line section of the permeation curve.

(9) Paul, D. R.; Koros, W. J. *J. Polym. Sci., Polym. Phys. Ed.* **1976**, *14*, 675.

(10) Fredrickson, G. H.; Helfand, E. *Macromolecules* **1985**, *18*, 2201.

(11) Barrer, R. M. *J. Membr. Sci.* **1984**, *18*, 25.

Hiroyuki Nishide, Hiroyoshi Kawakami,
Takayuki Suzuki, Yasutaka Azechi, and
Eishun Tsuchida*

Department of Polymer Chemistry
Waseda University, Tokyo 169, Japan

Received March 22, 1990
Revised Manuscript Received June 8, 1990